ARTICLE IN PRESS

Degradation of diphenhydramine pharmaceutical in aqueous solutions by using two highly active TiO$_2$ photocatalysts: Operating parameters and photocatalytic mechanism

Luisa M. Pastrana-Martínez[a], Joaquim L. Faria[a], José M. Doña-Rodríguez[b,*], Cristina Fernández-Rodríguez[b], Adrián M.T. Silva[a,*]

[a] LCM – Laboratory of Catalysis and Materials – Associate Laboratory LSRE/LCM, Faculdade de Engenharia, Universidade do Porto, Rua Dr. Roberto Frias, 4200-465 Porto, Portugal
[b] FEAM-Departamento de Química, Universidad de Las Palmas de Gran Canaria, Edificio Central del Parque Científico-Tecnológico de la ULPGC, Campus Universitario de Tafira, 35017 Las Palmas, Spain

ABSTRACT

In the present work the efficiency of a new TiO$_2$ catalyst (ECT), synthesized by means of an optimized sol–gel method, is studied for degradation of an important pharmaceutical water pollutant, diphenhydramine (DP). Its activity is compared to P25, the benchmark catalyst, produced by Evonik Degussa Corporation, under different catalyst loadings (up to 2.00 g L^{-1}) and initial solution pH (3.0–11.0). The results show that DP is very stable under non-catalytic conditions but complete degradation and considerable mineralization (ca. 60–70%) under near UV to visible irradiation ($\sim$50 mW cm^{-2}) can be achieved in 60 min by selecting the appropriate TiO$_2$ loading. ECT is significantly more active than the benchmark catalyst for loadings higher than 1.00 g L^{-1} while the pseudo-first order rate constant increased with the initial solution pH from 3.0 to 11.0. The highest rate constant was obtained with ECT at pH 11 (173 × 10^{-3} min^{-1} against 116 × 10^{-3} min^{-1} for P25). Scavenger agents were used as a diagnostic tool for the analysis of the photocatalytic mechanism and it was possible to prove that holes were crucial active species participating in the photocatalytic mechanism as well as that ECT has a higher availability than P25 to generate reactive radicals, such as hydroxyl (HO$^{\bullet}$) and hydroperoxyl (HOO$^{\bullet}$) radicals.

© 2011 Elsevier B.V. All rights reserved.

1. Introduction

Pharmaceutical active compounds (PACs) have attracted much attention in recent years due to their adverse effects towards natural organisms and potential effects on human beings. PACs are constantly released into aquatic environments mainly due to their widespread consumption and complicate removal in wastewater treatment plants. In fact, several studies in the past few years have demonstrated the presence of PACs in groundwater, surface water and even in drinking water [1–5].

Diphenhydramine (DP) hydrochloride, 2-(diphenylmethoxy)-N,N-dimethylethylamine hydrochloride, is the active ingredient of Benadryl® (and other PACs), a first generation antihistamine drug that combines sedative, antiemetic, antitussive and hypnotic properties. It is mainly used in the treatment of allergies, allergic rhinitis, hives, itching, insect bites and stings. The sedative and antiemetic properties of this pharmaceutical make it also efficient for the treatment of travel anxiety and travel sickness. DP works by blocking the influence of histamine at H$_1$ receptor sites, thus reducing the smooth muscle contraction. This drug is also used in many sleep aids [6]. The particular persistence of DP in natural waters is mainly related to its low biodegradability, and it has also shown high toxicity with mutagenic and carcinogenic effects [7].

Advanced oxidation processes (AOPs), based on the production and use of strongly reactive hydroxyl radicals, constitute promising technologies for the treatment of waters and wastewaters containing PACs [8–12]. DP degradation by UV and UV/H$_2$O$_2$ was already studied in combination with three other PACs (ibuprofen, phenazone, and phenytoin) [13]. DP was quite resistant to direct UV degradation and the obtained DP removal was less than 30% of the initial concentration when the UV treatment was assisted with H$_2$O$_2$.

Heterogeneous photocatalysis appears as one of the most destructive AOPs for organic contaminants, being possible to obtain the complete mineralization of organic pollutants into CO$_2$, water and inorganic ions, under ambient conditions and by using solar energy [14–16]. Titanium dioxide (TiO$_2$) is considered very close to an ideal semiconductor for photocatalysis due to its high efficiency and stability, low cost and safety [17]. However, at the best of

---

Table 1
Diphenhydramine hydrochloride properties.

Molecular formula	$C_{17}H_{21}NO \cdot HCl$
Molecular weight ($g\,mol^{-1}$)	291.82
Water solubility at 25 °C ($g\,L^{-1}$)	3.06
$\log K_{ow}$	3.27
pK_a	8.9

our knowledge, studies on the heterogeneous photocatalytic degradation of DP by using TiO_2 or any other photocatalyst were not reported yet.

The searching for extremely active TiO_2 catalysts under near UV–vis irradiation is nowadays a hot topic of research, one strategy being focused on tailoring the surface complexity, crystalline phase and size of these materials. There are several advantages on the synthesis of TiO_2 based photocatalysts through the sol–gel method, including the capability to fabricate very homogeneous powders with high photoactivity. For instance, the photocatalytic efficiency of a TiO_2 photocatalyst, recently developed by this method paying special attention to the sieving and calcination temperature (ECT-1023t, referred in the present work as ECT), showed phenol degradation rates 2.7 times higher than the benchmark TiO_2 photocatalyst from Evonik Degussa Corporation (P25) [18].

In this context, the present work is focused on the degradation of DP, under near UV–vis radiation, by testing this novel TiO_2 material (ECT) and the benchmark P25 photocatalyst. The main objective is to investigate the efficiency of these photocatalysts for DP degradation under different catalyst loadings and initial solution pH as well to conclude about the possible photodegradation mechanism for both materials by examination of active species through the use of scavengers for both radicals (tert-butanol, t-BuOH) and holes (ethylenediaminetetraacetic acid, EDTA).

2. Experimental

2.1. Chemicals

The high-purity analytical grade pharmaceutical specie selected for this study (DP) was supplied by Sigma–Aldrich (99% purity). The chemical structure of DP and its speciation diagram as function of pH, characterized by potentiometric titrations [19] are given in Supplementary Data (Fig. S1). Some characteristics of DP are listed in Table 1, where Kow is the octanol-water partition coefficient, a measure of hydrophobicity.

Potassium hydroxide (>90%) and tert-butanol (≥99.7%) were obtained from Fluka, Sigma–Aldrich. Hydrochloric acid (37%) was purchased from Pronolab. EDTA (>99%) was supplied by Fisher Scientific. Acetonitrile (≥99.8%) was used with HPLC grade (Chromanorm). Ultrapure water was produced in a Direct-Q millipore system.

2.2. Catalysts

Two TiO_2 catalysts were used in the study, a TiO_2 catalyst synthesized by means of a sol–gel procedure and fully characterized elsewhere, ECT-1023t (referred in the present work as ECT) [18], and the commercial P25 material, supplied by Degussa (now Evonik). Briefly, Table 2 summarizes the BET surface area (S_{BET}), relative amount of anatase and rutile crystalline phases and respective crystalline size, as well as the band-gap energy (E_{bg}) of both materials, as determined in a previous work [18]. In addition, the point zero of charge (pH_{PZC}) was determined as follows [20]: 50 mL of NaCl 0.01 M solution was placed in a closed Erlenmeyer flask. Then, the pH was adjusted to a value between 2 and 12 by adding HCl 0.1 M or NaOH 0.1 M, respectively, and 0.15 g sample of TiO_2 was added to each flask, the final pH being measured after 24 h

of continuous stirring at room temperature. The catalyst characterization indicates that ECT has a lower BET surface area, rutile content and band-gap energy than P25, while a larger crystalline size for both anatase and rutile phases and a slightly higher pH_{PZC} is characteristic of ECT when compared with P25.

2.3. Analytical techniques

The concentration of DP was analyzed by HPLC with a Hitachi Elite LaChrom system equipped with a Hydrosphere C18 column (250 mm × 4.6 mm; 5 μm particles), a Diode Array Detector (L-2450) and a solvent delivery pump (L-2130). An isocratic method set at a flow rate of 1 mL min^{-1} was used with the eluent consisting of an A:B (70:30) mixture of 20 mM NaH_2PO_4 acidified with H_3PO_4 at pH 2.80 (A) and acetonitrile (B). Absorbance was found to be linear over the whole range considered. The total organic carbon (TOC) was also determined for selected samples using a Shimadzu TOC-5000A analyzer. The maximum relative standard deviation of both HPLC and TOC measurements was never larger than 2%.

2.4. Photocatalytic experiments

The photocatalytic degradation of a 100 mg L^{-1} DP aqueous solution (3.40 × 10^{-4} mol L^{-1}) was carried out at room temperature (25 °C) under near UV to visible irradiation. The experiments were performed in a quartz cylindrical reactor filled with 7.5 mL of the model solution and the appropriate amount of TiO_2 was added to achieve the desirable catalyst loading (up to 2.00 g L^{-1}). The suspension was magnetically stirred and continuously purged with an oxygen flow. The irradiation source consisted in a Heraeus TQ 150 medium-pressure mercury vapor lamp (λ_{exc} = 254, 313, 366, 436 and 546 nm) and a DURAN® glass cooling jacket was used for obtaining irradiation in the near-UV to visible light range (λ_{exc} = 366, 436 and 546 nm) and to control the operating temperature. The lamp was positioned 6 cm away from the photoreactor. Irradiance at this position was approximately 50 mW cm^{-2}. Preliminary tests were performed with the aim to assess the reproducibility of the photocatalytic experiments in this reactor configuration, the relative error between repeated experiments being always lower than 5%.

Prior to irradiation, the suspension was magnetically stirred for 30 min in dark to establish the adsorption–desorption equilibrium that was confirmed for both P25 and ECT materials. The adsorption capacity was always lower than 4% of the initial DP concentration. After equilibration, the concentration of the substrate was measured and taken as the initial concentration (C_0) to discount the adsorption in the dark. At three intermediate time intervals and at the end of the experiment, small aliquots were sampled and immediately centrifuged at 14,000 rpm during 10 min to remove the catalyst particles. Reaction in the absence of catalyst was performed as a blank experiment in order to characterize direct photolysis. The experiments were performed at natural pH (5.4) and also at lower (3.0) and higher (7.0 and 11.0) pH.

The constant rate for the photocatalytic experiments can be modeled follow a pseudo-first order kinetic model, used in discussion of the mechanism of photocatalytic reaction in suspension systems [21–23]. The pseudo-first order kinetic model is described by the following equation:

$$C_{DP} = C_{DP,0}\, e^{-kt} \tag{1}$$

where k is the apparent kinetic constant of pseudo-first order, t is the reaction time and $C_{DP,0}$ and C_{DP} denote the DP concentrations at $t = 0$ and $t = t$ respectively.

For comparison, all the experimental conditions used in this study as well as the respective k constants obtained by fitting

Table 2
Characterization of P25 and ECT TiO$_2$ materials.

Catalyst	S_{BET} (m^2 g^{-1})	Crystalline phase (%)[a]	Crystalline size (nm)[a]	E_{bg} (eV)	pH$_{PZC}$
P25	52	80 (A)/20 (R)	22 (A)/25 (R)	3.18	6.3
ECT	18	89-94 (A)/11-6 (R)	57 (A)/86 (R)	2.97	7.1

[a] A: anatase; R: rutile.

the model described in Eq. (1) to the normalized DP concentration histories ($C_{DP}/C_{DP,0}$) are gathered in Table 3. The used Marquardt–Levenberg algorithm seeks the values of the parameters that minimize the sum of the squared differences between observed and predicted values of the dependent variable (the tolerance was set at 1×10^{-10}). Table 3 also shows the coefficient of variation, CV, expressed in percentage as k_{CV} (standard error $\times$ 100/parameter value), the standard error of each estimated k parameter (stderr) and the respective regression coefficient (r^2), in general indicating a good fitting of the model to the experimental data.

3. Results and discussion

3.1. Effect of catalyst loading on DP degradation

The selection of an optimal catalyst loading is of paramount importance in order to avoid excess of catalyst and to ensure a total absorption of efficient photons. The direct photolysis of DP aqueous solutions was first investigated in order to quantify the amount of DP degraded under non-catalytic conditions (hereafter referred as blank experiment). The photocatalytic degradation of DP at natural pH was also examined for different catalyst loadings and using both P25 and ECT catalysts (Figs. S2a and 2b, respectively, Supplementary Data). DP is very resistant to photodegradation under near-UV to visible light irradiation and natural pH (5.4) in the absence

of a catalyst, being obtained less than 6% of DP conversion in 60 min (Fig. S2a, Supplementary Data). DP degradation was found to increase with catalyst loading up to 0.25 g L^{-1} and 1.50 g L^{-1} for P25 and ECT, respectively, evidencing a heterogeneous regime. In both cases, complete photocatalytic DP degradation can be achieved in 60 min by selecting the appropriate amount of photocatalyst.

The respective k constants were determined (Table 3) and represented in Fig. 1. It is now clear that the reaction rate practically reached a plateau above a certain catalyst loading (i.e., the reaction rate become independent of the catalyst loading) which depends on the TiO$_2$ material used. It is well known that active sites increase with the catalyst loading and that after a certain loading part of the catalyst surface is unavailable for effective absorption of photons [24–26]. The optimal loading depends on the photoreactor geometry and operating conditions, but Fig. 1 shows an additional dependence with respect to the TiO$_2$ material used.

Therefore, the P25 catalyst is very efficient for low catalyst loadings ($k = 12.2 \times 10^{-3}$, 22.9×10^{-3}, 56.7×10^{-3} and 55.9×10^{-3} min^{-1} or 7.68×10^{-3}, 13.1×10^{-3}, 30.0×10^{-3} and 51.3×10^{-3} min^{-1} for 0.03, 0.05, 0.25 and 0.50 g L^{-1} of P25 or ECT, respectively) but higher degradation rates can be obtained with ECT at catalyst loadings equal or higher than 1.00 g L^{-1} ($k = 56.3 \times 10^{-3}$, 62.9×10^{-3} and 64.7×10^{-3} min^{-1} or 59.1×10^{-3}, 76.7×10^{-3} and 77.7×10^{-3} min^{-1} for 1.00, 1.50 and 2.00 g L^{-1} of P25 or ECT, respectively).

Table 3
Pseudo-first order kinetic rate constant (k) of DP degradation under different experimental conditions and respective coefficient of variation (CV), expressed as a percentage (k_{CV}), standard error (stderr) and regression coefficient (r^2). Bold parameters in a column means a set of experiments performed varying the respective parameter while keeping the others constant.

| Catalyst	C_{cat} (g L^{-1})	Initial pH	Scavenger	$k \times 10^{-3}$ (min^{-1})	k_{CV} (%)	stderr $\times 10^{-3}$ (min^{-1})	r^2
None	**0**	5.4	None	1.00	6.9	0.07	0.9504
P25	**0.03**	5.4	None	12.2	2.0	0.2	0.9977
P25	**0.05**	5.4	None	22.9	2.6	0.6	0.9969
P25	**0.25**	5.4	None	56.7	2.2	1.2	0.9990
P25	**0.50**	5.4	None	55.9	2.7	1.5	0.9983
P25	**1.00**	5.4	None	56.3	5.3	3.0	0.9938
P25	**1.50**	5.4	None	62.9	3.1	2.0	0.9979
P25	**2.00**	5.4	None	64.7	4.1	2.6	0.9967
ECT	**0.03**	5.4	None	7.68	2.8	0.22	0.9504
ECT	**0.05**	5.4	None	13.1	3.1	0.4	0.9947
ECT	**0.25**	5.4	None	30.0	3.0	0.9	0.9938
ECT	**0.50**	5.4	None	51.3	6.9	0.4	0.9964
ECT	**1.00**	5.4	None	59.1	1.3	0.4	0.9999
ECT	**1.50**	5.4	None	76.7	1.1	0.9	0.9996
ECT	**2.00**	5.4	None	77.7	1.7	1.3	0.9999
None	0	**7.0**	None	1.95	1.7	0.03	0.9975
None	0	**11.0**	None	3.77	9.4	0.35	0.9079
P25	1.00	**3.0**	None	29.7	4.5	1.3	0.9932
P25	1.00	**7.0**	None	71.7	0.8	0.6	0.9999
P25	1.00	**11.0**	None	116	4.7	5.5	0.9976
ECT	1.00	**3.0**	None	47.5	1.0	0.5	0.9997
ECT	1.00	**7.0**	None	58.7	5.1	2.3	0.9943
ECT	1.00	**11.0**	None	173	6.0	10.4	0.9978
P25	0.50	5.4	**EDTA**	4.74	11.0	0.52	0.9320
P25	0.50	5.4	**tBuOH**	24.3	1.8	0.4	0.9986
ECT	0.50	5.4	**EDTA**	1.99	4.3	0.09	0.9825
ECT	0.50	5.4	**tBuOH**	18.4	3.5	0.6	0.9935
P25	1.00	11.0	**EDTA**	7.86	2.3	0.18	0.9964
P25	1.00	11.0	**tBuOH**	73.9	2.1	1.6	0.9991
ECT	1.00	11.0	**EDTA**	3.77	4.8	0.18	0.8788
ECT	1.00	11.0	**tBuOH**	43.6	1.8	0.8	0.9990
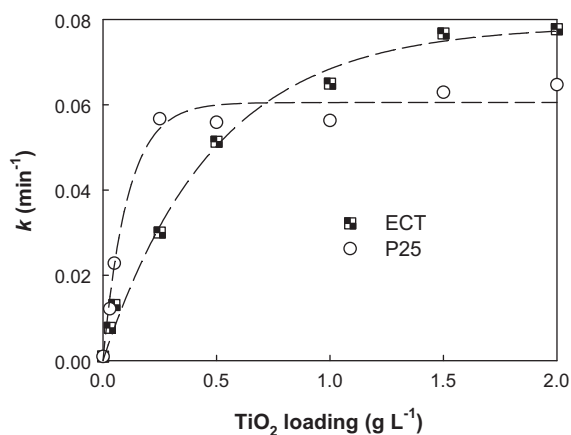
Fig. 1. Pseudo-first order reaction rate constant (k) for different catalyst loadings of P25 and ECT photocatalysts at natural pH (5.4).

Fig. 2. Pseudo-first order reaction rate constant (k) for different initial solution pH when P25 and ECT photocatalysts are used at fixed catalyst loading of $1.00\,\text{g\,L}^{-1}$.

3.2. Effect of solution pH on DP degradation

In the photocatalytic reactions, pH is an important parameter affecting the efficiency of degradation process since it influences the surface charge properties of the catalyst, the charge of the organic molecules and the concentration of hydroxyl radicals (HO•).

The respective k constants of DP photolysis within 60 min of irradiation at different pH values can be found in Table 3. The direct photolysis alone degraded a negligible amount of DP at natural pH ($k = 1.00 \times 10^{-3}\,\text{min}^{-1}$) and only a slight increase of the pseudo-first order reaction rate constant was observed for DP degradation by increasing the initial solution pH ($k = 1.95 \times 10^{-3}$ and $3.77 \times 10^{-3}\,\text{min}^{-1}$ for pH of 7.0 and 11.0, respectively), which corresponds to less than 20% of DP degradation.

The speciation diagram of DP (Fig. S1, Supplementary Data) shows the relevant equilibrium between the protonated (DP^+) and deprotonated (DP) forms of diphenhydramine, pK_a representing the acid dissociation constant. This diagram shows that the protonated form is the only specie at pH values below 7.0. The deprotonated form appears at higher pH due to deprotonation of the amine group ($pK_a = 8.9$) and is the solely specie observed at pH values above 11.0.

In photocatalytic experiments, the TiO_2 surface charge density is affected by the pH medium [27,28], and thus, different electrostatic interactions between diphenhydramine and the catalyst will occur when working at different pH according to the following water equilibrium equations:

$$TiOH + H^+ \rightleftharpoons TiOH_2^+ \tag{2}$$

$$TiOH + OH^- \rightleftharpoons TiO^- + H_2O \tag{3}$$

At the natural solution pH (5.4) the protonated form of DP (DP^+) is the specie contained in the solution while the surface of the TiO_2 materials used in the present study will be positively charged according to their pH_{PZC}.

The experiments performed varying the initial pH of the DP solution at a fixed catalyst loading of $1\,\text{g\,L}^{-1}$ are shown in Figs. S3a and S3b (Supplementary Data), respectively for P25 and ECT photocatalysts. This loading was selected because similar reaction rates were observed at this catalyst loading for both TiO_2 materials (Fig. 1) and because this loading is the one typically used in photocatalytic experiments at the literature. DP degradation is markedly affected by the pH of the initial solution. Both catalysts are able to enhance the photodegradation of DP regardless of the pH used. In addition, the efficiency of the photocatalytic process increases with the initial solution pH. This effect seems to be critical when using ECT at the highest pH tested, as can be observed on
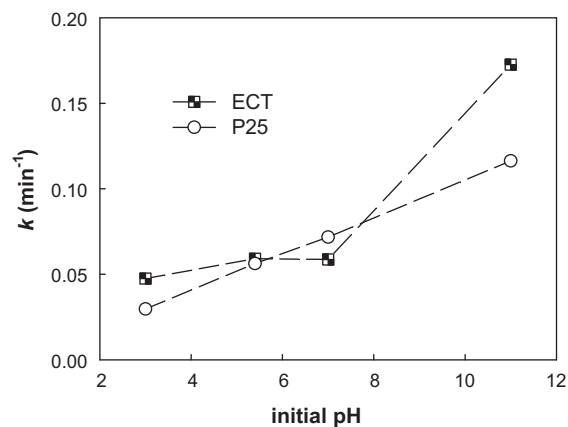
Fig. 2, where the respective k constants (Table 3) are represented for the different pH. A linear increase of k with the pH was observed for P25, as already reported for the photocatalytic degradation of phenolic compounds with this photocatalyst [15], but the linear correlation was not found for ECT.

The reaction rate constant decreased for both TiO_2 materials when the solution pH was decreased from the natural pH of 5.4 ($k = 56.3 \times 10^{-3}$ and $59.1 \times 10^{-3}\,\text{min}^{-1}$ for P25 and ECT, respectively) to 3.0 ($k = 29.7 \times 10^{-3}$ and $47.5 \times 10^{-3}\,\text{min}^{-1}$ for P25 and ECT, respectively). This can be explained by the increased electrostatic repulsions between the catalyst surface that is positively charged as $TiOH_2^+$ (Eq. (2)) and the positive charge of DP^+ at these conditions (Fig. S1, Supplementary Data). Other possible explanations are that the catalyst tends to agglomerate under acidic conditions, being reduced the available surface area for DP adsorption and photon absorption [28], or even that chlorine species from HCl could compete with the organic compounds for the photogenerated oxidative species [29].

At pH 7.0 the electrostatic attraction of DP to the P25 catalyst (pH_{PZC} 6.3, Table 2) is expected as a result of the DP^+ positive charge ($pK_a = 8.9$, Fig. S1, Supplementary Data) and the negatively charged catalyst surface (Eq. (3)). For ECT (pH_{PZC} 7.1, Table 2), the electrostatic attraction of the DP^+ positive charge should be weaker than for P25 at pH 7.0, probably explaining the lower k constant obtained for ECT ($58.7 \times 10^{-3}\,\text{min}^{-1}$) when compared with P25 ($71.7 \times 10^{-3}\,\text{min}^{-1}$) at this pH (Table 3).

In fact, the highest photodegradation rate was obtained for both materials at pH of 11.0 (116×10^{-3} and $173 \times 10^{-3}\,\text{min}^{-1}$ for P25 and ECT, respectively). Since the pH_{PZC} of P25 and ECT are 6.3 and 7.1, respectively, their surfaces will be negatively charged at such alkaline conditions (Eq. (3)). Therefore, the marked enhancement on the photodegradation rate should be attributed to the presence of more hydroxyl anions at these conditions, leading to a larger amount of hydroxyl radicals formed at the catalyst surface by the reaction of hydroxyl anions with positive holes (Eq. (4)) [22,30,31], and as consequence to a higher DP degradation (66% and 83% for P25 and ECT, respectively, only after 10 min of reaction).

$$h_{vb}^+ + HO^- \rightarrow HO^\bullet \tag{4}$$

In addition, only a slight decrease on the pH was observed after the photocatalytic experiments, never larger than 0.5 (e.g., from 5.4 to 5.0 at natural solution pH; from 3.1 to 2.7 at initial pH 3.0; from 7.0 to 6.5 at initial pH 7.0; and from 11.1 to 10.7 at initial pH 11.0). This decrease is not significant but seems to indicate that low molecular weight carboxylic acids were formed during the reaction.
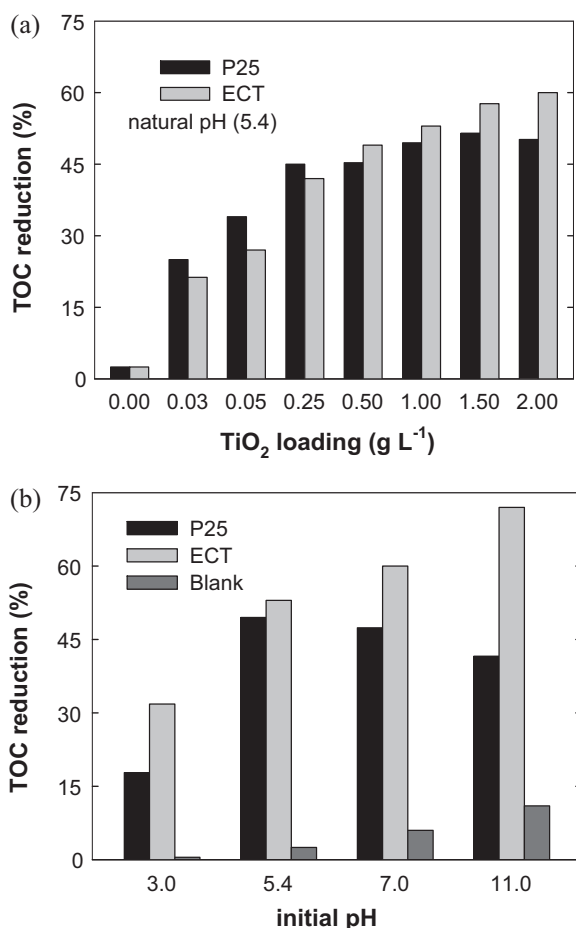
Fig. 3. Total organic carbon (TOC) reduction for different loadings of P25 and ECT photocatalysts at natural solution pH (a) and for different initial solution pH in the presence and absence of $1.00\,g\,L^{-1}$ of P25 and ECT photocatalysts (b).

3.3. Effect of catalyst loading and solution pH on DP mineralization

Regarding the mineralization monitored by measuring the TOC, Fig. 3a shows the TOC reduction for the different catalyst loadings at natural pH at the end of the experiments (60 min of reaction). As expected, the photodegradation experiment in the absence of catalyst leads to a negligible TOC reduction (2.5%). In general the TOC reduction follows the trends observed for DP degradation in the photocatalytic experiments (Fig. 1), and TOC reductions of up to 60% can be achieved depending on the implemented catalyst and respective loading. It is of special interest to note that higher mineralization levels where obtained with ECT, in comparison with P25, when the catalyst loading was equal or higher than $0.50\,g\,L^{-1}$. Therefore, the performance of both materials is comparable at such natural conditions, being the ECT material more efficient than P25 at higher catalyst loadings in terms of both DP degradation (Fig. 1) and mineralization (Fig. 3a).

The TOC reduction was also determined for the photocatalytic experiments performed with different initial pH at fixed catalyst loading of $1.00\,g\,L^{-1}$. Fig. 3b shows the obtained results together with those obtained in the absence of catalyst. The level of mineralization during photolysis increases with the solution pH but was never higher than 11%. The TOC reduction for P25 found a maximum at the natural pH. In contrast, when using the ECT catalyst, the mineralization is enhanced by increasing the initial solution pH (32, 53, 60 and 72% for initial pH of 3.0, 5.4, 7.0 and 11.0, respectively), as also observed for DP degradation (Fig. 2).
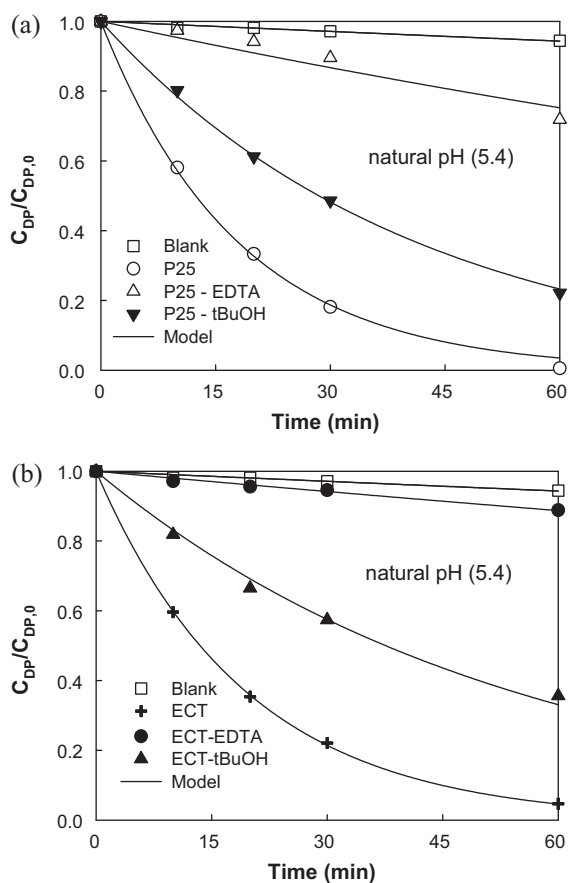

Fig. 4. Effect of holes/radicals scavengers (EDTA/t-BuOH) on the photocatalytic degradation of DP with $0.50\,g\,L^{-1}$ catalyst loading at natural pH for P25 (a) and ECT (b). Curves represent the fitting of the pseudo-first order equation to the experimental data.

Therefore, the mineralization efficiency (Fig. 3b) and DP degradation (Fig. 2) increase with the initial pH for ECT. Additionally, DP degradation also increases when a higher pH was tested for P25 (Fig. 2). There is only a different trend to this behavior: the mineralization obtained with P25 decreases with the increase of the initial pH (Fig. 3b for pH > 5.4). This result can be explained by different reaction pathways occurring at low and high pH, the intermediate compounds that are formed at high pH being more difficult to be oxidized than those formed at low pH.

3.4. Effect of holes/radicals scavengers (EDTA/t-BuOH)

Oxidative species generated in photocatalytic process can be detected through trapping experiments of holes and radicals, by adding excess of EDTA or t-BuOH, respectively [32,33]. Experiments were repeated by using these scavengers ($10\,mmol\,L^{-1}$) for two selected conditions, namely at pH of 11 at fixed catalyst loading of $1.0\,g\,L^{-1}$, corresponding to the experiment where the higher DP and TOC degradation were achieved in the present study, and at natural pH and catalyst loading of $0.50\,g\,L^{-1}$, corresponding to typical operating conditions where both catalysts showed comparable performance.

For the later situation, Fig. 4a and b show the normalized DP concentration histories when P25 and ECT where used, respectively. For P25 (Fig. 4a), the presence of t-BuOH (radicals scavenger) leads to a considerable change on the profile of DP degradation and to a marked decrease of the pseudo-first order rate constants ($k = 55.9 \times 10^{-3}$ and $24.3 \times 10^{-3}\,min^{-1}$ in the absence and presence of t-BuOH, respectively), but this change is more notorious in

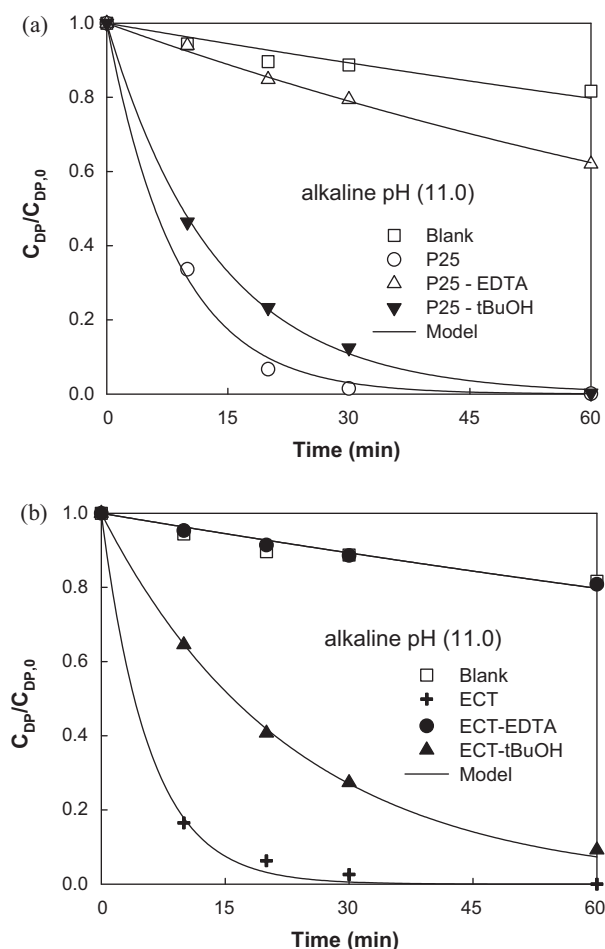**Fig. 5.** Effect of holes/radicals scavengers (EDTA/t-BuOH) on the photocatalytic degradation of DP with $1.0\,g\,L^{-1}$ catalyst loading at pH of 11.0 for P25 (a) and ECT (b). Curves represent the fitting of the pseudo-first order equation to the experimental data.

the presence of EDTA ($k = 4.74 \times 10^{-3}\,min^{-1}$), showing that even if reactive radicals, such as hydroxyl (HO•) and hydroperoxyl (HOO•) radicals, are responsible species for part of the photocatalytic oxidation reaction, photogenerated holes on the catalyst surface (h^+) seems to be the major active species participating on the degradation process. The photodegradation of DP in the presence of EDTA and t-BuOH was also investigated for the ECT catalyst (Fig. 4b). In this case the k constants decreased from $51.3 \times 10^{-3}\,min^{-1}$ in the absence of any scavenger to 18.4×10^{-3} and $1.99 \times 10^{-3}\,min^{-1}$ in the presence of t-BuOH and EDTA, these values being comparable to those obtained for P25.

In order to obtain a better picture of the photocatalytic mechanism, the same methodology was applied to the experiments at pH of 11 and fixed catalyst loading of $1.0\,g\,L^{-1}$ (Fig. 5a and b, for P25 and ECT, respectively). For P25 the k constant decreases from $116 \times 10^{-3}\,min^{-1}$ in the absence of the scavengers to 73.9×10^{-3} and $7.86 \times 10^{-3}\,min^{-1}$ in the presence of t-BuOH and EDTA, respectively, while for ECT the respective decrease takes place from $173 \times 10^{-3}\,min^{-1}$ in the absence of scavengers to 43.6×10^{-3} and $3.77 \times 10^{-3}\,min^{-1}$ in the presence of t-BuOH and EDTA, respectively (Table 3).

Therefore, it seems that, for both TiO_2 photocatalysts, the photogenerated holes (h^+) play an important role on the mechanism of DP degradation, regardless of the pH media, while the extremely high activity found for ECT at the highest pH tested (Fig. 2) seems to be associated to the higher availability of ECT to generate

reactive radicals at these conditions, such as hydroxyl (HO•) and hydroperoxyl (HOO•) radicals, in comparison with P25, since the inhibition of the degradation reaction that takes place by these radicals was evidently more significant for ECT (k decreases from 173×10^{-3} to $43.6 \times 10^{-3}\,min^{-1}$) than for P25 ($k$ decreases from $116 \times 10^{-3}\,min^{-1}$ to $73.9 \times 10^{-3}\,min^{-1}$) when t-BuOH was added to the reaction system.

4. Conclusions

ECT is a very active catalyst for degradation and mineralization of the DP pharmaceutical, its catalytic activity being even higher than the one observed with the benchmark photocatalyst (P25) when the catalyst load is higher than $1.00\,g\,L^{-1}$. In general, the pseudo-first order rate constants increased with catalyst loading until a certain value where the activity reach a plateau, evidencing an heterogeneous regime, and also with the initial solution pH, mainly attributed to enhanced formation of the reactive hydroxyl radicals at the catalyst surface. Photogenerated holes are the main responsible species in the catalytic degradation of DP when using both P25 and ECT materials, but ECT has a higher availability than P25 to generate highly reactive hydroxyl (HO•) and hydroperoxyl (HOO•) radicals, as proved in experiments performed with a scavenger for holes (EDTA) and a scavenger for radicals (t-BuOH).

Acknowledgements

Appendix A. Supplementary data

Supplementary data associated with this article can be found, in the online version, at doi:10.1016/j.apcatb.2011.11.041.

References

[1] O.A. Jones, J.N. Lester, N. Voulvoulis, Trends in Biotechnology 23 (2005) 163–167.
[2] Y. Valcárcel, S.G. Alonso, J.L. Rodríguez-Gil, R.R. Maroto, A. Gil, M. Catalá, Chemosphere 82 (2011) 1062–1071.
[3] J. Radjenovic, M. Petrovic, F. Ventura, D. Barceló, Water Research 42 (2008) 3601–3610.
[4] A. Kumar, I. Xagoraraki, Science of The Total Environment 408 (2010) 5972–5989.
[5] M.J. Focazio, D.W. Kolpin, K.K. Barnes, E.T. Furlong, M.T. Meyer, S.D. Zaugg, L.B. Barber, M.E. Thurman, Science of The Total Environment 402 (2008) 201–216.
[6] BP' 2005, British Pharmacopoeia, The Stationary Office on behalf of the Medicines and Healthcare Products Regulatory Agency (MHRA), 2005.
[7] C.A. Kinney, E.T. Furlong, S.L. Werner, J.D. Cahill, Environmental Toxicology and Chemistry 25 (2006) 317–326.
[8] M. Klavarioti, D. Mantzavinos, D. Kassinos, Environment International 35 (2009) 402–417.
[9] F.L. Rosario-Ortiz, E.C. Wert, S.A. Snyder, Water Research 44 (2010) 1440–1448.
[10] F.J. Benitez, J.L. Acero, F.J. Real, G. Roldan, F. Casas, Chemical Engineering Journal 168 (2011) 1149–1156.
[11] A. Ziylan, N.H. Ince, Journal of Hazardous Materials 187 (2011) 24–36.
[12] F. Méndez-Arriaga, T. Otsu, T. Oyama, J. Gimenez, S. Esplugas, H. Hidaka, N. Serpone, Water Research 45 (2011) 2782–2794.
[13] F. Yuan, C. Hu, X. Hu, J. Qu, M. Yang, Water Research 43 (2009) 1766–1774.
[14] M.N. Chong, B. Jin, C.W.K. Chow, C. Saint, Water Research 44 (2010) 2997–3027.
[15] A.M.T. Silva, E. Nouli, N.P. Xekoukoulotakis, D. Mantzavinos, Applied Catalysis B: Environmental 73 (2007) 11–22.
[16] S. Malato, J. Blanco, A. Vidal, C. Richter, Applied Catalysis B: Environmental 37 (2002) 1–15.

[17] A. Fujishima, T.N. Rao, D.A. Tryk, Journal of Photochemistry and Photobiology C: Photochemistry Reviews 1 (2000) 1–21.

[18] J. Araña, J.M. Doña-Rodríguez, D. Portillo-Carrizo, C. Fernández-Rodríguez, J. Pérez-Peña, O. González Díaz, J.A. Navío, M. Macías, Applied Catalysis B: Environmental 100 (2010) 346–354.

[19] L.M. Pastrana-Martínez, M.V. López-Ramón, C. Moreno-Castilla, Journal of Colloid and Interface Science 331 (2009) 2–7.

[20] J. Rivera-Utrilla, I. Bautista-Toledo, M.A. Ferro-García, C. Moreno-Castilla, Journal of Chemical Technology & Biotechnology 76 (2001) 1209–1215.

[21] B. Ohtani, Journal of Photochemistry and Photobiology C: Photochemistry Reviews 11 (2010) 157–178.

[22] P. Jantawasu, T. Sreethawong, S. Chavadej, Chemical Engineering Journal 155 (2009) 223–233.

[23] A.O. Ibhadon, G.M. Greenway, Y. Yue, P. Falaras, D. Tsoukleris, Applied Catalysis B: Environmental 84 (2008) 351–355.

[24] F. Méndez-Arriaga, S. Esplugas, J. Giménez, Water Research 42 (2008) 585–594.

[25] J.M. Herrmann, Catalysis Today 24 (1995) 157–164.

[26] I.K. Konstantinou, T.A. Albanis, Applied Catalysis B: Environmental 49 (2004) 1–14.

[27] A.-G. Rincón, C. Pulgarin, Applied Catalysis B: Environmental 51 (2004) 283–302.

[28] M.A. Fox, M.T. Dulay, Chemical Reviews 93 (1993) 341–357.

[29] E.P. Paola Calza, Pure and Applied Chemistry 73 (2001) 1839–1848.

[30] C. Galindo, P. Jacques, A. Kalt, Journal of Photochemistry and Photobiology A: Chemistry 130 (2000) 35–47.

[31] Z. Shourong, H. Qingguo, Z. Jun, W. Bingkun, Journal of Photochemistry and Photobiology A: Chemistry 108 (1997) 235–238.

[32] N. Serpone, I. Texier, A.V. Emeline, P. Pichat, H. Hidaka, J. Zhao, Journal of Photochemistry and Photobiology A: Chemistry 136 (2000) 145–155.

[33] C. Minero, G. Mariella, V. Maurino, D. Vione, E. Pelizzetti, Langmuir 16 (2000) 8964–8972.